ChemComm

Fast and reversible solvent-vapor-induced 1D to 2D transformation in emissive Ag(I)-organic networks

Journal:	*ChemComm*
Manuscript ID	CC-COM-07-2023-003540.R1
Article Type:	Communication

Chemical Communications

COMMUNICATION

Fast and reversible solvent-vapor-induced 1D to 2D transformation in emissive Ag(I)-organic networks

Received 00th January 20xx,
Accepted 00th January 20xx

DOI: 10.1039/x0xx00000x

www.rsc.org/

Maxim I. Rogovoy,[a] Mariana I. Rakhmanova,[a] Evgeniy H. Sadykov,[a] Gia M. Carignan,[b] Irina Yu. Bagryanskaya,[c] Jing Li,[b]* Alexander V. Artem'ev[a]*

We report here an unprecedentedly fast and reversible transformation between 1D and 2D MOFs/CPs induced through organic solvent vapours. The transformations occur at room temperature in just 15–20 min, accompanied by a significant change in the observed phosphorescence. These findings provide a new insight in the design of luminescent networks with stimuli-switchable dimensionality.

One-, two- and three-dimensional (1D, 2D, 3D) metal-organic frameworks (MOFs) or coordination polymers (CPs) have attracted increasing attention owing to their unique properties, which demonstrate potential for a variety of applications in diverse fields.[1-3] A higher lability of the metal-ligand bonds (24–72 kcal·mol^{-1}),[4, 5] compared to the covalent ones (24–190 kcal·mol^{-1}), allows MOFs to be ideal materials for studying dimensional transformations (1D to 2D, 2D to 3D, 1D to 3D, or vice versa), which offer an enormous possibility to construct new advanced materials.[6-8] On this account, development and understanding of dimensional transformations is an extremely important research component in MOF science.[9] One of the strategies for the change in framework dimensionality is based on organic reactions between neighboring ligands. However, despite some value,[7, 8] this approach often suffers from irreversibility of the reactions and is limited by access to the specific ligands. Modification of the metal's environment by removal of coordinated molecules *via* external stimuli is a much more powerful strategy to realize a number of dimensional transformations. Most of which, however, are unreversible.[6-8] While reversible dimensional transformations have been reported for various MOFs,[10] they typically require high temperature and/or elongated time for one or both stages.[11-14] For example, 1D MOF [Pb_2(8-Quin)$_2$(NO_3)$_2$(MeOH)] (8-HQuin = 8-hydroxyquinoline) upon heating at 165–170 °C polymerizes into 2D MOF [Pb(8-Quin)(NO_3)], which can be again converted back to the 1D MOF by soaking in MeOH.[15] In another work,[16] 1D MOF [Co(bpy)(OTf)$_2$(H_2O)$_2$] was transformed into 2D MOF [Co(bpy)$_2$(OTf)$_2$] by heating at 125 °C for 2 h, whilst the reverse process was accomplished by immersion of the latter into CH_3CN for 10 days. Another reversible network transformation was recently reported by Kitagawa et al.[17] for 1D-[Cu(BDC)(H_2O)$_2$]·H_2O and 2D-[Cu(BDC)DMF] (bdc = 1,4-benzenedicarboxylate), where 1D-to-2D reaction was realized in DMF at 100 °C for 18 days, and the reverse process took place in water for 12 h. The reversible dimensional transformations occurring at ambient temperature and with high rate for both stages, to our knowledge, are unprecedented.

Herein, we showcase a remarkably fast and reversible transformation between 1D and 2D Ag(I)-based MOFs induced by exposing to organic solvent vapours at 20–25 °C for just 15–20 mins. A noticeably bright and different phosphorescence of these MOFs allowed us to investigate the structure transformation dynamics in real time.

The two MOFs, 1D-[Ag_3L_2(CH_3CN)$_2$(OTf)$_3$] (**1**) and 2D-[Ag_3L_2(OTf)$_3$] (**2**), were synthesized in high yield by treating AgOTf with diphenyl(2-pyrimidyl)phosphine (L) in CH_3CN and CH_2Cl_2 medium, respectively (for details, see §3 in ESI†). The polymeric fragments and building units of **1** and **2** are depicted in Figure 1. Both structures contain a basic unit {Ag_2L_2}, in which two Ag atoms are bridged by two L ligands (μ_2-P,N) in a head-to-tail manner to provide Ag···Ag contacts as short as 2.9865(7) and 3.1946(5) Å in **1** and **2**, respectively (*cf.* twice Bondi's VdW radius of Ag, 3.44 Å). In both MOFs, the {Ag_2L_2} units are linked by μ_2-OTf anions into 1D {Ag_2L_2–(μ_2-OTf)}$_n$ subarrays; the Ag–O distances in **1** are of 2.476 and 2.642 Å, and 2.392 Å in **2**. In polymer **1**, these 1D subarrays are coupled by means of [Ag(μ_2-OTf)(κ_1-OTf)] crosspieces into two-wire 1D chains. In the latter, the Ag3 atom is bonded with pyrimidine N atom of one

[a] Nikolaev Institute of Inorganic Chemistry, Siberian Branch of Russian Academy of Sciences, 3, Acad. Lavrentiev Ave., 630090 Novosibirsk, Russia
[b] Department of Chemistry and Chemical Biology, Rutgers University, Piscataway, New Jersey 08854, United States
[c] Vorozhtsov Novosibirsk Institute of Organic Chemistry, Siberian Branch of Russian Academy of Sciences, 9, Acad. Lavrentiev Ave., 630090 Novosibirsk, Russia
*Authors for correspondence: chemisufarm@yandex.ru (Alexander V. Artem'ev) jingli@rutgers.edu (Jing Li)
†Electronic Supplementary Information (ESI) available: [general details, synthesis and characterization data, PXRD patters, FT-IR spectra, TGA curves, photophysical and computational data]. CCDC 2208215, 2208216. See DOI: 10.1039/x0xx00000x

subarray, while the O atom of the μ_2-OTf anion is coordinated with Ag1 atom of the neighbouring subarray ($d_{Ag–O}$ = 2.66 Å). The Ag2 and Ag3 atoms of **1** are also ligated by MeCN molecules ($d_{Ag–NCMe}$ = 2.547 and 2.205 Å, respectively), thereby adopting a seesaw four-coordinated geometry. In the packing, 1D chains of **1** are propagated along the *a* axis and, along this direction, they look like hollow roboid tubes. In polymer **2**, the $\{Ag_2L_2–(\mu_2\text{-}OTf)\}_n$ subarrays are combined into zig-zag shaped 2D layers through cross-linking with $Ag(\kappa_1\text{-}OTf)_2$ units, in which the metal adopts a rare square-planar $Ag@N_2O_2$ geometry. Similarly, the 2D layers of **2** are expanded along the *a* axis.

Phase purity of MOFs **1** and **2** was confirmed by powder X-ray diffraction (PXRD, Figs. S1, S2†) and microanalysis data. As thermogravimetric (TG) and PXRD data suggested, in the 87–108 °C range, 1D chains of **1** lose the coordinated MeCN molecules and transform into 2D sheets of **2**, which stay stable up to 340 °C (Fig. S3†).

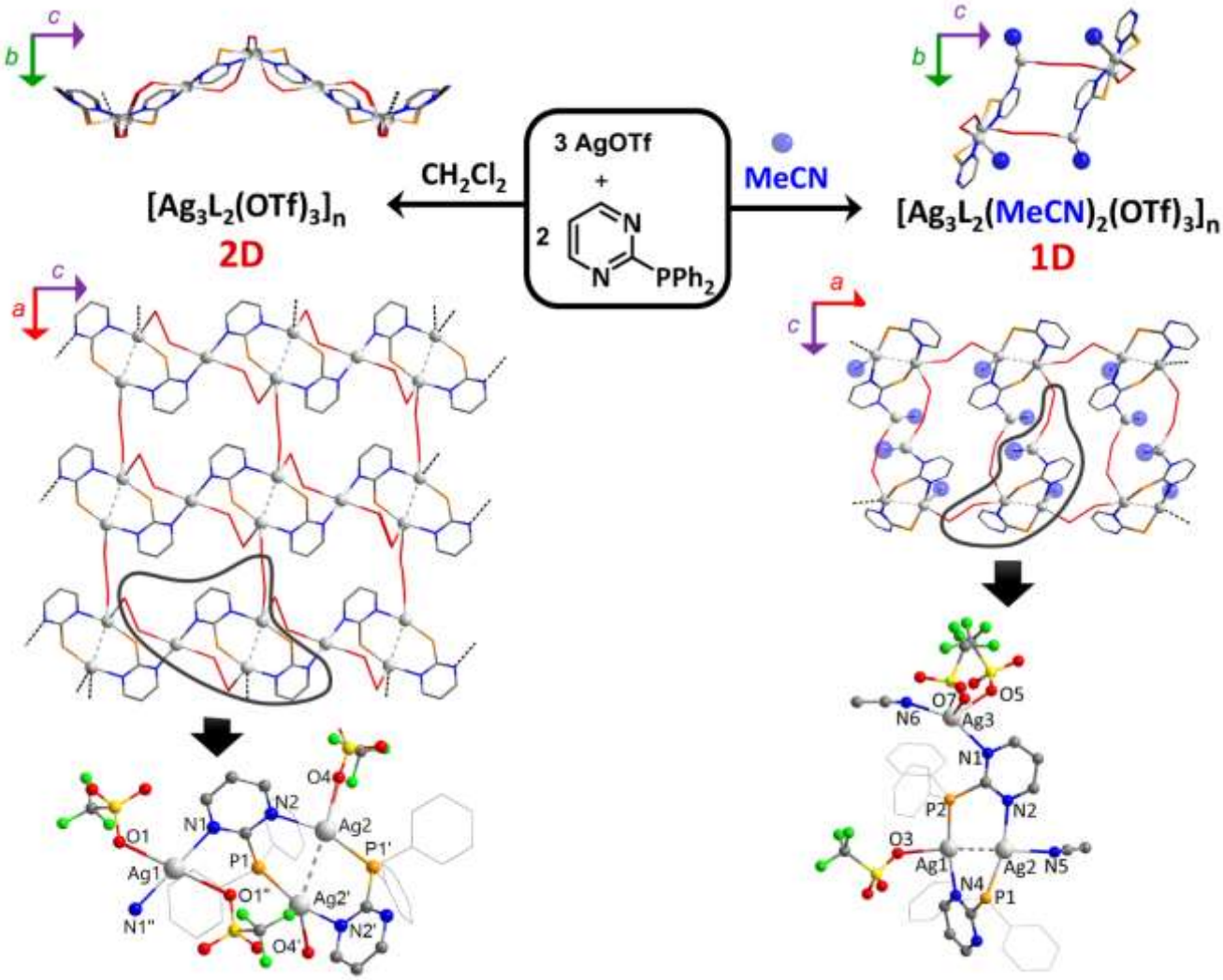

Fig. 1. Genesis and structures of 1D and 2D MOFs, $[Ag_3L_2(CH_3CN)_2(OTf)_3]$ (**1**) and $[Ag_3L_2(OTf)_3]$ (**2**). The CH_3CN ligands in the chains of **1** are shown as bluish balls. Symmetry codes for **2**: (') 1–*x*, *y*, 3/2–*z*; ('') 1–*x*, 1–*y*, 1–*z*.

At room temperature, MOFs **1** and **2** emit very bright phosphorescence (RTP) in the cyan and sky-blue region with high quantum efficiencies of 65 and 48%, respectively. In these terms, both compounds out-perform the majority of known Ag(I)-based MOFs, which commonly demonstrate a weak photoluminescence. The emission spectra of **1** and **2** reveal bands with λ_{max} = 503 and 471 nm, respectively, whose broad shape indicates a charge-transfer emission (Fig. 2a). The afterglow times at 298 K being 62 μs for **1**, and 47 μs for **2** indicate a relatively fast rate of RTP with the radiative rates (k_r) of 10^4 s^{-1} order. Upon gradual cooling from 298 to 77 K, the emission spectra show band intensification and shifting of the maxima to longer wavelengths by 677–861 cm^{-1}. At that, the afterglow times of **1** and **2** increase by 3–4 times only, amounting to 187 and 174 μs at 77 K. The long afterglow times, large Stokes shift (8100–8700 cm^{-1}) as well as the non-TADF (thermally activated delayed fluorescence)-specific shape of the decay time against temperature plots [τ(T), Fig. S7†], clearly point to a triplet emission origin for both studied frameworks throughout the 77–298 K range.

In order to understand the origin of phosphorescence in **1** and **2**, we carried out DFT calculations to obtain their electronic

band structures and projected densities of states (§9; ESI†). Based on the projected density of states (PDOS) analysis, it is clear the atomic states that contribute to the valence band maximum (VBM) of **1** and **2** are a mixture of both ligand components and the AgOTf component, while the atomic states in the conduction band minimum (CBM) are primarily from the ligand. More specifically, for compound **1**, the largest contributions to the VBM are from Ag 4d, O 2p from OTf anions and the C 2p of the ligand (Fig. S8†).

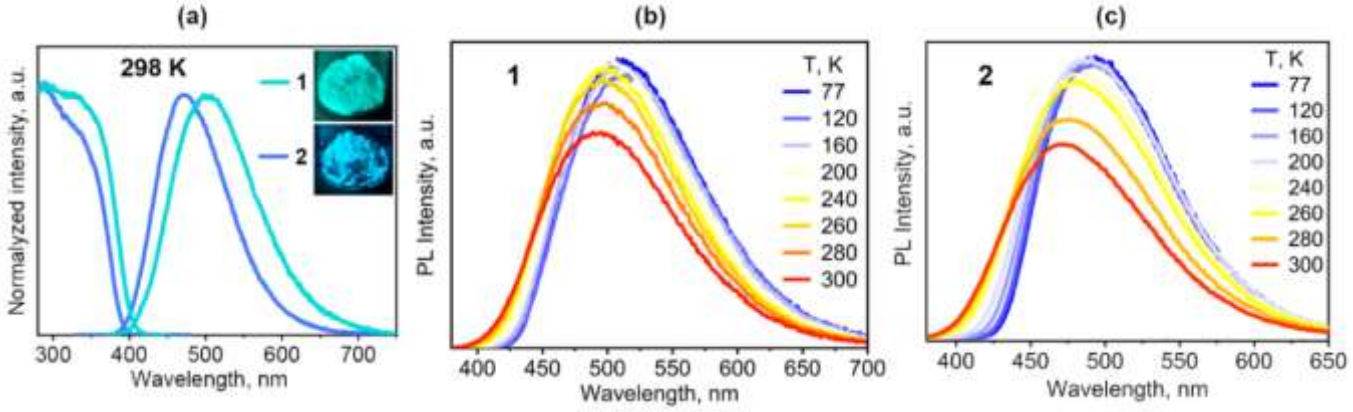

Fig. 2. (a) Emission spectra of solid **1** and **2** (*Insert:* UV-irradiated powders of these compounds); (b) Temperature-depended emission spectra of **1** (λ_{ex} = 300 nm); (c) Temperature-depended emission spectra of **2** (λ_{ex} = 300 nm).

Compound **2** also has a significant contribution from the F 2p orbital of OTf-anion (Fig. S9†). Comparably, the ligand contributions to the very top levels of the VBM have a higher percentage in polymer **1** than in **2**. The CBM of both polymers is mostly made up of the C 2p of the ligand with smaller contributions from N 2p. In the case of polymer **1**, the coordinated MeCN molecules do not have an appreciable contribution to neither the CBM nor VBM. Thus, phosphorescence of **1** and **2** can be assigned to ^{3}(MLCT) and ^{3}IL mixed type (X = OTf, IL is intraligand). Note that the (M+X)LCT emission was previously reported for some Ag(I)-based emitters,[18] just as intraligand phosphorescence.[19]

MOFs **1** and **2** were found to undergo fast and reversible 1D ↔ 2D solid-to-solid transformation that is induced by solvent vapors under mild conditions (23–25°C). To the best of our knowledge, there has been only one report of a solvent vapor-induced reversible dimensional transition between a 1D and a 3D MOF, which progressed at low speed (39 h and 1 week, respectively).[11] A pronounced difference in the emission properties of **1** and **2** makes it possible to track dynamics of both 1D-to-2D and 2D-to-1D interconversions (Fig. 3). Upon fuming powder **1** with CH_2Cl_2 vapor for merely 15 min, its 1D chains are quantitatively cross-linked into 2D layers of **2**. During the reaction, emission color of the powder smoothly changes from cyan to sky blue (**see video file VD1**). Spectrally, this transformation is accompanied by a gradual decrease in the emission intensity and shift of its maximum from 503 and 471 nm (Fig. 3b). Apparently, CH_2Cl_2 vapour gradually condenses on the surface of **1** and causes the elimination of CH_3CN ligands from the 1D chains which, in becoming MeCN-free, are cross-linked into 2D layers of **2**. Note that the transformation of **1** to **2** can also be induced by $CHCl_3$, CCl_4, acetone, MeOH, and benzene vapors, albeit at a slower rate (PXRD data; for details, see §11 in ESI†). The emission intensity versus time plot (Fig. 3b, insert) reveals a gradual intensity decrease during the 1D → 2D reaction. This fact is consistent with a lower quantum yield of **2**, and also indicates a single-stage character of the process. Reversely, the 2D sheets of **2** can be easily and quantitatively converted into 1D chains of **1** by fuming with CH_3CN vapor for just 20 min (Fig. 3c). Herein, the 1D → 2D transformation is demonstrated by a gradual shift of the band from 470 to 504 nm, occurring through an initial drop and subsequent increase in integral intensity (Fig. 3c, inset). Visually, this appears as a gradual change in the emission color from sky-blue to cyan (**see video file VD2**).

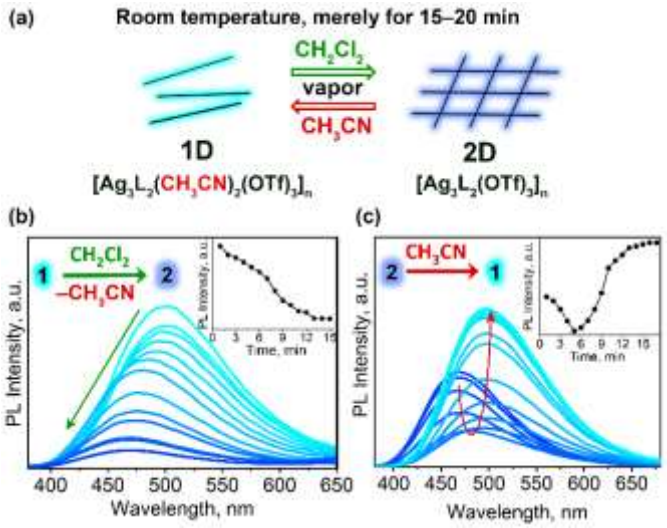

Fig. 3. (a) Solvent-vapor-induced 1D ↔ 2D transformations; (b) Evolution of the emission spectra during 1D → 2D solid-state reaction (λ_{ex} = 300 nm); (c) Evolution of the emission spectra during 2D → 1D solid-state reaction (λ_{ex} = 300 nm).

The above results agree well with PXRD and microanalysis data, confirming conversion for the above transformations at 15–20 min. The PXRD patterns of recovered MOFs **1** and **2** are comparable with those of parent samples (Figs. S10, S11†).

Remarkably, a dry filter paper impregnated with polymer **1** (as depicted in Figure 4a) quickly and reversibly changes the emission color upon fuming with CH_2Cl_2 vapor. The fabricated paper under daylight is of white color, whilst the impregnation sites show cyan emission like polymer **1** (Fig. 4b). As demonstrated in Figure 4b and supplemented move (**see video file VD3**), immersing the fabricated paper in CH_2Cl_2 vapor for merely 2–3 s gradually leads to a visible disappearance of the cyan emissive sites. Even more surprising is that the cyan emission of the impregnation sites reappears almost instantly when the paper is removed from the CH_2Cl_2 vapors. Overall, the disclosed "on-off" process is repeatable. These observations can be tentatively explained by CH_2Cl_2-induced transformation of **1** into **2** on the paper surface. Because the UV-irradiated paper itself has nearly the same blue color as emission chromaticity of **2**, the **1** → **2** transformation looks like a disappearance of cyan-emitting spots. The MeCN released in this process is possibly somehow retained in the paper and reacts again with **1** under CH_2Cl_2-free atmosphere. Naturally, a deeper explanation of this phenomenon requires a special study, which is beyond the scope of this communication.

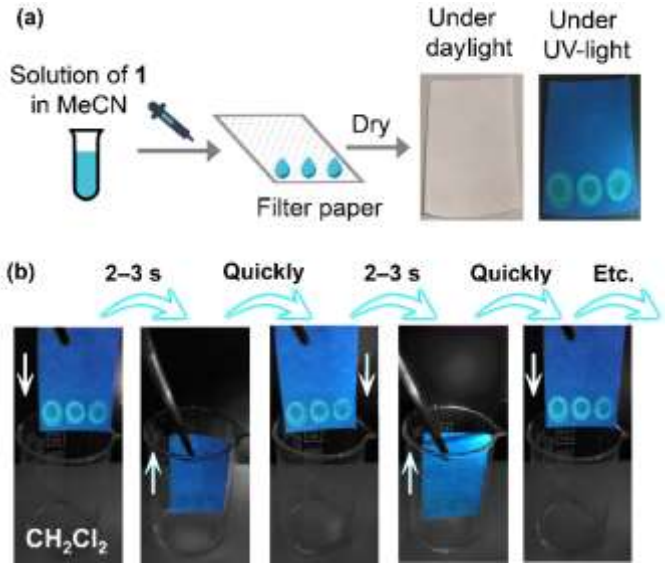

Fig. 4. (a) Preparation of a sensing paper based on **1**; (b) Reversible change in emission during immersion and removal of a sensing paper into a bottle with a CH_2Cl_2 vapor (25 °C, under 365 nm light).

In summary, a reversible vapochemical 1D to 2D transformation between emissive Ag(I)-based MOFs is discovered to occur with an unprecedently fast rate at ambient temperature. This reaction significantly differs from previously observed transformations of MOFs. Despite a major rearrangement of the entire structure and packing, both stages are triggered simply by solvent vapors, and these stages occur very fast under clearly mild conditions. Moreover, a noticeably bright RTP of the 1D and 2D MOFs allowed us to explore their interconversion dynamics by emission spectroscopy in real time. At the fundamental level, our findings contribute to the crystal engineering of MOFs and provide new possibilities for the design of new materials, the dimensionality of which can be quickly and reversibly switched by external stimuli. From a practical viewpoint, the constructed MOFs can be considered as potential vapochemical sensors[20] and stimuli-responsive triplet emitters.

Conflicts of interest

There are no conflicts to declare.

Acknowledgements

This work was supported by Russian Science Foundation (Project №21-73-10110) and the Ministry of Science and Higher Education of the Russian Federation (Projects №121031700321-3, №121031700313-8 and 1021051503141-0-1.4.1). The Rutgers team would like to acknowledge the partial support by U.S. Department of Energy, Office of Science, Office of Basic Energy Sciences through Grant No. DE-SC0019902.

References

1. H. Furukawa, K. E. Cordova, M. O'Keeffe and O. M. Yaghi, *Science*, 2013, **341**, 1230444.
2. D. N. Dybtsev and K. P. Bryliakov, *Coord. Chem. Rev.*, 2021, **437**, 213845.
3. A. A. Lysova, D. G. Samsonenko, K. A. Kovalenko, A. S. Nizovtsev, D. N. Dybtsev and V. P. Fedin, *Angew. Chem. Int. Ed.*, 2020, **59**, 20561-20567.
4. C.-H. Li and J.-L. Zuo, *Adv. Mater.*, 2020, **32**, 1903762.
5. O. M. Yaghi, *J. Am. Chem. Soc.*, 2016, **138**, 15507-15509.
6. G. K. Kole and J. J. Vittal, *Chem. Soc. Rev.*, 2013, **42**, 1755-1775.
7. G. Chakraborty, I.-H. Park, R. Medishetty and J. J. Vittal, *Chem. Rev.*, 2021, **121**, 3751-3891.
8. W.-W. He, S.-L. Li and Y.-Q. Lan, *Inorg. Chem. Front.*, 2018, **5**, 279-300.
9. C.-P. Li, J. Chen, C.-S. Liu and M. Du, *Chem. Comm.*, 2015, **51**, 2768-2781.
10. C. Hu and U. Englert, *Angew. Chem. Int. Ed.*, 2005, **44**, 2281-2283.
11. S. Nakatsuka, Y. Watanabe, Y. Kamakura, S. Horike, D. Tanaka and T. Hatakeyama, *Angew. Chem. Int. Ed.*, 2020, **59**, 1435-1439.
12. S. M. Mobin, A. K. Srivastava, P. Mathur and G. K. Lahiri, *Dalton Trans.*, 2010, **39**, 8698-8705.
13. J. Campo, L. R. Falvello, I. Mayoral, F. Palacio, T. Soler and M. Tomás, *J. Am. Chem. Soc.*, 2008, **130**, 2932-2933.
14. J.-Y. Wu, C.-Y. Chang, C.-J. Tsai and J.-J. Lee, *Inorg. Chem.*, 2015, **54**, 10918-10924.
15. A. Aslani and A. Morsali, *Chem. Comm.*, 2008, **2008**, 3402-3404.
16. A. Kondo, T. Nakagawa, H. Kajiro, A. Chinen, Y. Hattori, F. Okino, T. Ohba, K. Kaneko and H. Kanoh, *Inorg. Chem.*, 2010, **49**, 9247-9252.
17. Y. Jing, Y. Yoshida, P. Huang and H. Kitagawa, *Angew. Chem. Int. Ed.*, 2022, **61**, e202117417.
18. H. Yersin, R. Czerwieniec, M. Z. Shafikov and A. F. Suleymanova, *ChemPhysChem*, 2017, **18**, 3508-3535.
19. M. I. Rogovoy, A. S. Berezin, D. G. Samsonenko and A. V. Artem'ev, *Inorg. Chem.*, 2021, **60**, 6680-6687.
20. H. Wang, W. P. Lustig and J. Li, *Chem. Soc. Rev.*, 2018, **47**, 4729-4756.